Superlattice dislocations and magnetic transition in Fe-Al alloys with the B2-type ordered structure

1991 J. Phys.: Condens. Matter 3 5805

(http://iopscience.iop.org/0953-8984/3/31/004)

J. Phys.: Condens. Matter 3 (1991) 5805–5816. Printed in the UK

Superlattice dislocations and magnetic transition in Fe–Al alloys with the B2-type ordered structure

S Takahashi† and Y Umakoshi‡

† Faculty of Engineering, Iwate University, Morioka 020, Japan

‡ Department of Materials Science and Engineering, Faculty of Engineering, Osaka University, Suita 565, Japan

Received 16 October 1990, in final form 8 April 1991

Abstract. Magnetization was measured in plastically deformed 34.0, 36.2 and 40.0 at.% Al–Fe alloys with the B2 structure in the temperature range from 77 K to room temperature. At 34.0 at.% Al concentration, the spontaneous magnetization, M_s, increases considerably as a result of 4% strain and has a broad maximum at about 200 K, which would result in mictomagnetism. The Fe–Al alloys containing 36.2 and 40.0 at.% Al are paramagnetic before plastic deformation and as a result of plastic deformation the magnetic susceptibility, χ, increases remarkably and at the same time M_s appears. The Curie temperature, T_C, becomes higher with increasing strain. Superlattice dislocations were observed by use of an electron microscope. A [111] superlattice dislocation is separated into two (1/2) [111] superpartials coupled by a ribbon of antiphase boundary (APB). The APB width is 28 to 35 nm. The dislocation density, ρ, is 10^9 to 10^{10} cm^{-2}. The relation between M_s amd ρ which is calculated by a simple localized moment model is compared with the experimental results. The change of T_C and the increase of χ suggest the existence of a long-range influence between ferromagnetic clusters as far as 10^2 nm.

1. Introduction

Iron–aluminum alloys are ideal materials to use to study the effect of the atomic environment on magnetic properties; the observed changes in their intrinsic magnetic properties could be correlated with atomic rearrangements associated with order–disorder processes and with Al concentrations. In Fe_3Al alloys with the DO_3 structure, the Fe atom with eight Fe atoms at the nearest neighbour (NN) sites carries the magnetic moment of 2.2 μ_B, while the Fe atom with four Fe and four Al atoms at the NN sites carries the moment of 1.5 μ_B. The spontaneous magnetization decreases rapidly with the excess Al concentrations, and beyond 35 at.% Al the phase is no longer spontaneously ferromagnetic. Although Fe–Al alloys containing Al contents more than 35 at.% are paramagnetic in the B2 structure, they become ferromagnetic in disordered samples heavily deformed by crushing. The above two magnetic transitions are associated with the change of the atomic configuration (Huffman and Fisher 1967, Kouvel 1969, Beck 1971, Besnus *et al* 1975). The magnetic transitions have been explained from the viewpoint of the local atomic environment by many investigators. The magnetic moment of the host Fe atom depends on the number of Al atoms (n_{Al}) at the first NN sites. The magnetic

0953-8984/91/315805 + 12 $03.50

moment of the Fe atom is fairly constant at 2.2 μ_B when $n_{Al} \leqslant 2$. The moment becomes 1.5 μ_B at $n_{Al} = 4$ and finally reaches zero at $n_{Al} \geqslant 5$.

Huffman and Fisher (1967) introduced a simple model to explain the experimental results of magnetic transition due to plastic deformation; the plastic deformation induces a large number of antiphase boundaries (APB), in the vicinity of which the atomic configuration changes in NN. The area of the APB increases with plastic deformation in proportion to the dislocation density, ρ, and the spontaneous magnetization, M_s, can be represented as a simple function of ρ (Takahashi 1986). One of the purposes of the present study is to examine experimentally the relationship between M_s and ρ.

Most investigators used powder specimens, disordered by crushing or grinding. It would be difficult to obtain accurate information about atomic rearrangement after plastic deformation because of the complex nature and the distribution of dislocations. The change of atomic configuration due to cold work can be controlled by tensile deformation with small plastic strain. Recently some interesting phenomena due to plastic deformation were found in Fe–Al alloys (Takahashi and Umakoshi 1990b): the Curie temperature becomes higher with increasing plastic strain, ε, and the magnetic susceptibility, χ, increases considerably with a few percent strain. The phenomena seem difficult to explain by only the local atomic environment effects depending on n_{Al}. Detailed experimental results are shown in this paper.

2. Experimental procedure

Fe–Al alloys were melted in an argon arc furnace from 99.9% Fe and 99.99% Al. The single crystal rods were prepared by the Bridgman technique and the chemical compositions of these alloys were 34.0, 36.2 and 40.0 at.% Al by EDX analysis. They were homogenized at 1273 K for one day in vacuum. They were cooled very slowly at the rate of 30 K per day from 973 K to room temperature to obtain a high degree of the B2-type ordered structure. Rectangular prisms ($50 \times 2.5 \times 2.5$ mm^3) were cut out from a single crystal rod. The specimens were tested in tension at room temperature by an Instron-type machine. The specimens for magnetic measurement ($2 \times 2 \times 2.5$ mm^3) were cut out from the rectangular prisms by the Servomet spark machine, and their surface damage was removed by chemical polishing. Magnetic measurements were made on a balance suitable for measuring the susceptibility of paramagnetic specimens in the temperature range from 77 K to 300 K. Thin-foil specimens for electron microscopy were also prepared from the rectangular prisms by spark machining and finally thinned by the electrochemical polishing method. The thin foils were examined in an H-800 electron microscope operating at 200 kV.

3. Experimental results

3.1. Magnetic measurements

Magnetic measurements were made in a range of magnetic field strength between 0.84×10^5 and 9.8×10^5 A m^{-1} at temperatures from 77 K to room temperature. Figure 1 shows the isothermal magnetization curves for the specimens before and after plastic deformation in 40.0 and 36.2 at.% Al contents. After plastic deformation, the magnetization increases at every temperature compared with the undeformed results. Variations of the magnetization with applied magnetic field are found to yield straight lines except for the low-field range where the deviation of magnetization from a straight

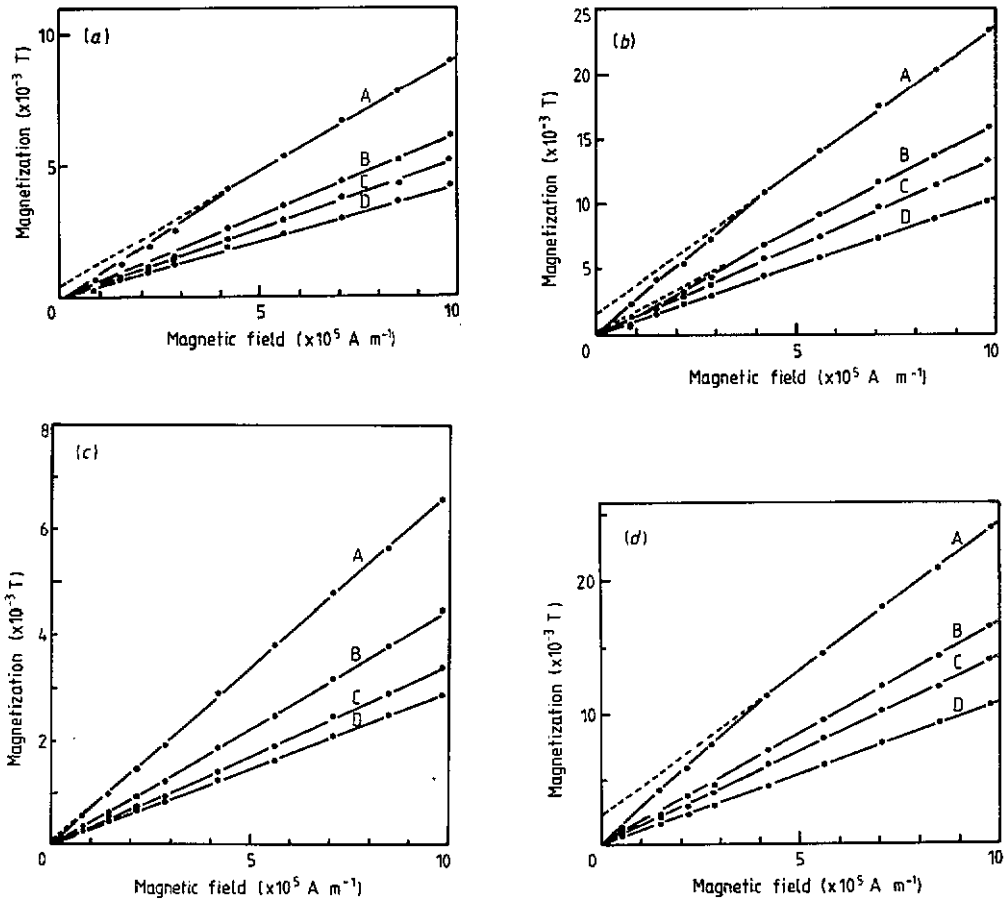

Figure 1. The variation of magnetization with applied magnetic field at different temperatures for 40 at.% Al–Fe alloy at (*a*) $\varepsilon = 0\%$, (*b*) $\varepsilon = 5\%$ and for 36.2 at.% Al–Fe alloy at (*c*) $\varepsilon = 0\%$ and (*d*) $\varepsilon = 5.5\%$. The curves are as follows: A, 77 K; B, 130 K; C, 165 K; D, 273 K.

line occurs in the curves. The values of M_s and χ are obtained from the linear parts of magnetization curves by a least-squares fit to the isothermal magnetic data. The extrapolation back to zero field of the linear parts is shown by the broken lines in figure 1.

In the 34.0 at.% Al content alloy a ferromagnetic magnetization process is observed even before plastic deformation. The applied magnetic field of 10^6 A m^{-1} is not enough to make the magnetization curve completely saturated as shown in figure 2. M_s and χ are obtained above 5.6×10^5 A m^{-1}.

The susceptibility of 40.0 and 36.2 at.% Al content alloy is plotted as a function of the reciprocal of test temperatures in figure 3. χ increases with increasing strain and χ for the sample deformed to $\varepsilon = 5\%$ attains to a value three times as large as that before plastic deformation at 77 K.

The variation of M_s with temperature in 40.0 at.% Al content alloy is shown in figure 4. The uncertainties in M_s due to the instability of test temperature are shown by error bars. M_s appears even in a slightly deformed sample and increases with increasing

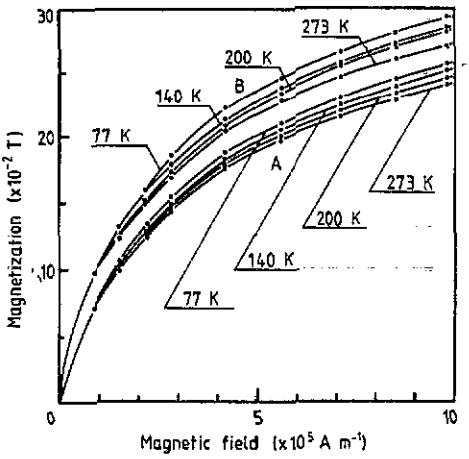

Figure 2. The variation of magnetization with applied magnetic field at different temperatures for 34.0 at.% Al–Fe alloy at (A) $\varepsilon = 0\%$ and (B) $\varepsilon = 7.5\%$.

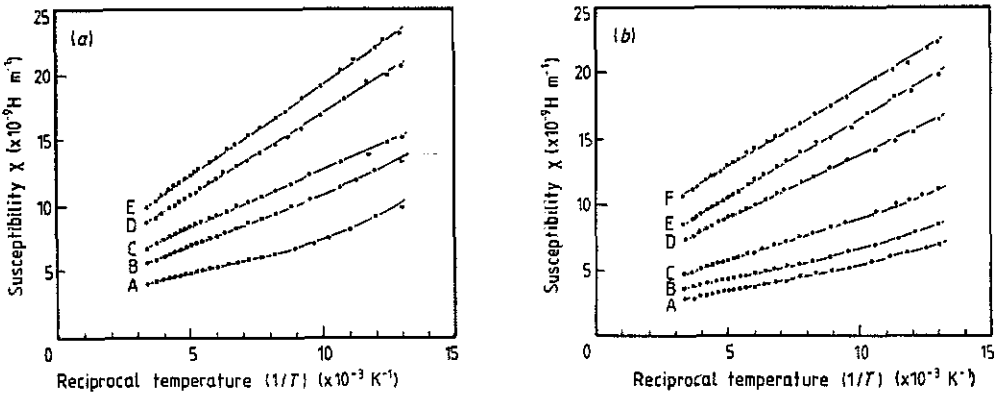

Figure 3. The variation of susceptibility χ with the reciprocal temperatures. (*a*) for 40.0 at.% Al–Fe alloy: A, $\varepsilon = 0\%$; B, $\varepsilon = 1.6\%$; C, $\varepsilon = 2\%$; D, $\varepsilon = 3.5\%$; E, $\varepsilon = 5.0\%$; F, $\varepsilon = 5.5\%$. (*b*) for 36.2 at.% Al–Fe alloy: A, $\varepsilon = 0\%$; B, $\varepsilon = 1.5\%$: C, $\varepsilon = 2.0\%$; D, $\varepsilon = 3.5\%$: E, $\varepsilon = 5.0\%$: F, $\varepsilon = 5.5\%$.

strain. The values of M_s decrease rapidly as the temperature increases and disappear at temperature T_C. T_C becomes high with increasing plastic strain and becomes higher than room temperature at 13% strain.

Figure 5 shows the variation of M_s with temperature in 36.2 at.% Al content alloy. The variation of M_s is somewhat similar to that of 40.0 at.% Al content below $\varepsilon = 5\%$. Above $\varepsilon = 5\%$ the value of M_s increases more rapidly with increasing plastic strain than that of 40.0 at.% Al content (see figure 4). M_s in 34.0 at.% Al content alloy is shown versus the test temperature in figure 6. The increase of M_s due to plastic deformation is very large compared with the other Al content alloys and M_s has a broad maximum at about 200 K, though any M_s-temperature peak does not appear in the undeformed specimens. No significant change of χ due to plastic deformation has been observed in the 34.0 at.% alloy.

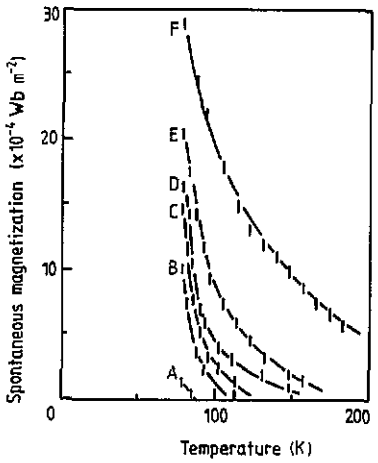

Figure 4. The variation in the spontaneous magnetization due to plastic deformation for 40.0 at.% Al–Fe alloy: curve A, $\varepsilon = 1.6\%$; B, $\varepsilon = 3\%$; C, $\varepsilon = 4\%$; D, $\varepsilon = 5.1\%$; E, $\varepsilon = 6\%$; F, $\varepsilon = 13\%$.

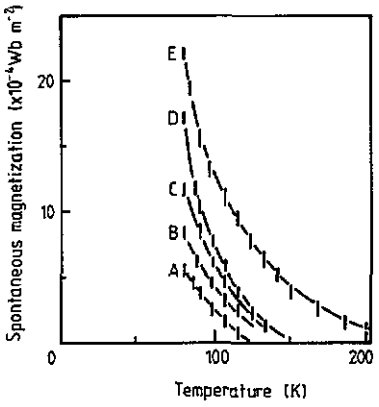

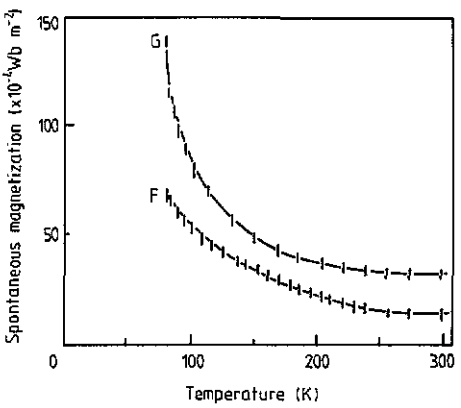

Figure 5. The variation in the spontaneous magnetization due to plastic deformation for 36.2 at.% Al–Fe alloy: curve A, $\varepsilon = 1.5\%$; B, $\varepsilon = 2.0\%$; C, $\varepsilon = 3.5\%$; D, $\varepsilon = 5.0\%$; E, $\varepsilon = 5.5\%$; F, $\varepsilon = 8.0\%$; G, $\varepsilon = 9.5\%$.

3.2. Electron microscopy observation

The fully ordered B2 structure was confirmed from electron diffraction patterns. No antiphase domain was observed since the B2 structure is stable up to the melting point. The superlattice dislocation in Fe–Al alloys with the B2 structure has been studied by several investigators (Leamy *et al* 1969, Umakoshi and Yamaguchi 1980). Figures 7(*a*) and 7(*b*) are the electron micrographs of specimens with 1.6% strain in 40.0 at.% Al content alloy. Figure 7(*a*) shows a weak-beam image of the dissociation of a [111] superlattice dislocation into two (1/2) [111] superpartial dislocations. Almost superpartials make a pair and the separation of superlattice dislocations is 28 to 35 nm on the

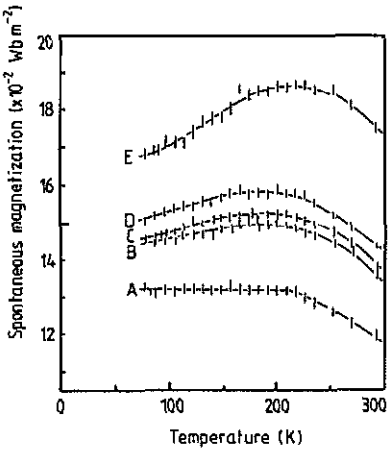

Figure 6. The variation of spontaneous magnetization with temperature for 34.0 at.% Al–Fe alloy: A, $\varepsilon = 0\%$; B, $\varepsilon = 2.2\%$; D, $\varepsilon = 4.0\%$; E, $\varepsilon = 7.5\%$.

{110} plane. The thickness of the foil is estimated to be about 100 nm by counting the number of thickness fringes from the edge of the specimen. The dislocation density, ρ was measured by counting the intersection of dislocation lines with straight lines drawn at random on photographic films. The observed dislocation density may include about 30% errors which come from the uncertainty of foil thickness and the diffraction condition. Also $\rho = 2 \times 10^9\ \mathrm{cm}^{-2}$ at $\varepsilon = 1.6\%$. ρ increases with increasing strain and it becomes $7 \times 10^9\ \mathrm{cm}^{-2}$ at $\varepsilon = 5.1\%$ as shown in figure 7(*c*). Figures 8(*a*) and 8(*b*) are the electron micrographs of specimens with 1.5% and 7% strain in 36.2 at.% Al content alloy. Superpartials distribute with a pair, whose separation is 30 to 35 nm. ρ increases from 2.5×10^9 to $1.1 \times 10^{10}\ \mathrm{cm}^{-2}$ with strain increasing from 1.5% to 7%. Figure 9 is the electron micrograph of 34.0 at.% Al content alloy with 4% strain where ρ is $6 \times 10^9\ \mathrm{cm}^{-2}$. Paired superpartial dislocations are observed and many independent superpartials are also recognized.

4. Superlattice dislocations and magnetic transition

In the B2-type structure of $Fe_{(1+c)}Al_{(1-c)}$ with $0 \leqslant c \leqslant 0.5$, there are two different sites; the α sites (corner sites) are occupied only by Fe atoms and the β sites (body centred sites) are randomly occupied by Al and Fe atoms (in a stoichiometric Fe–Al ordered alloy, the β sites are occupied only by Al atoms). The leading superpartial dislocation creates an APB on the {110} glide plane after it has slipped. In the vicinity of the APB, the arrangement of Fe and Al atoms is different from that in the ordered state. Table 1 shows n_{Al} around the host Fe atoms before and after plastic deformation. The host α- and β-site Fe atoms have different n_{Al} in the vicinity of the APB from that in the normal state at the NN.

Figure 10 shows the schematic arrangement of the α-site Fe atoms in the vicinity of the APB on the (110) glide plane. The atomic plane is the $(\bar{1}10)$ being perpendicular to the glide plane. In the vicinity of the APB, the α-site Fe atoms are arranged in a chain with their first NN in the [001] direction. According to the electron micrographs, the

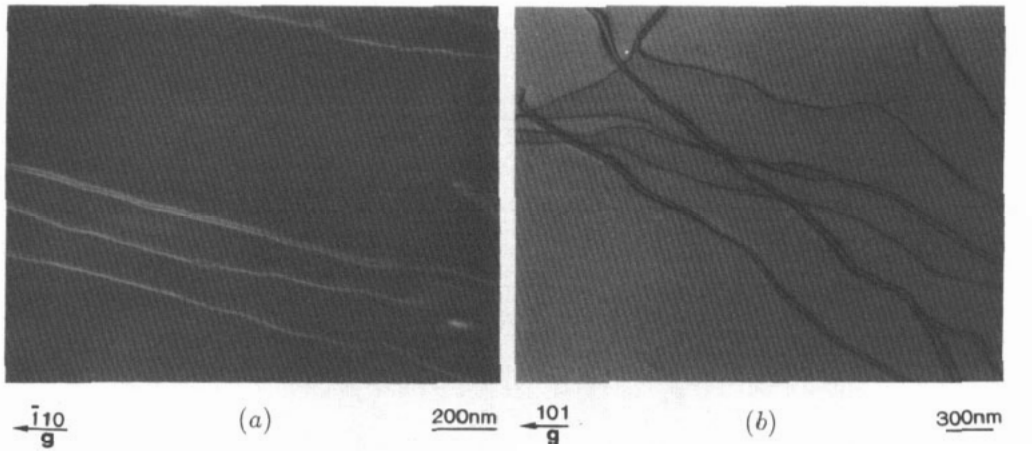

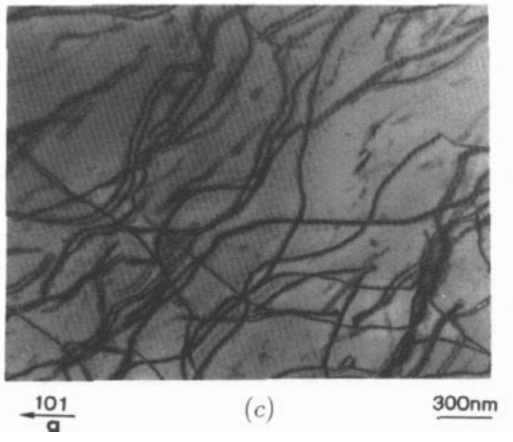

Figure 7. The electron micrographs of 40.0 at.% Al–Fe single crystals: (*a*) the weak-beam image of the dissociation of a [111] superlattice dislocation at $\varepsilon = 1.6\%$; (*b*) $\varepsilon = 1.6\%$; (*c*) $\varepsilon = 5.1\%$.

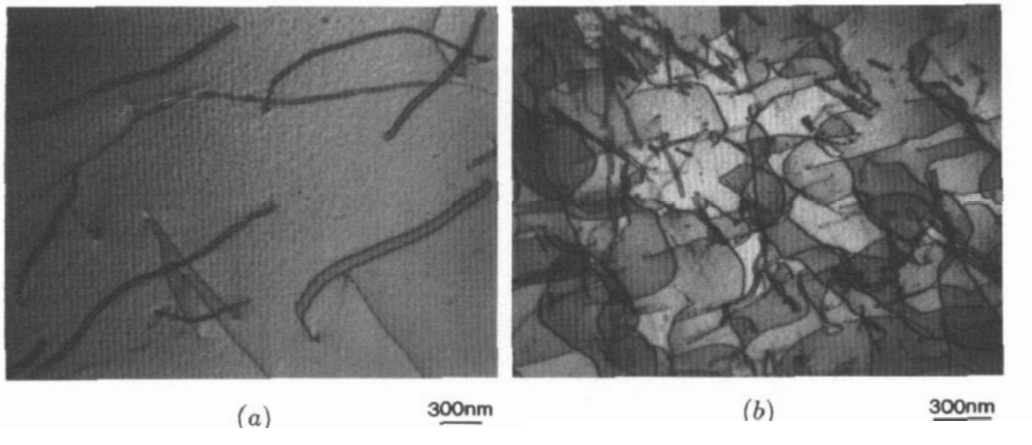

Figure 8. The electron micrographs of 36.2 at.% Al–Fe single crystals: (*a*), $\varepsilon = 1.5\%$; (*b*), $\varepsilon = 7.0\%$.

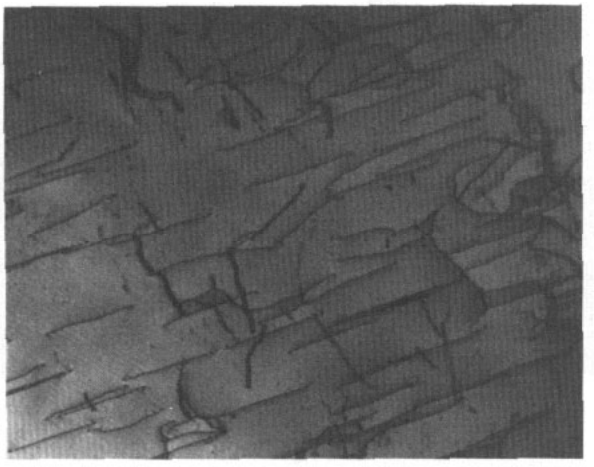

Figure 9. The electron micrograph of 34.0 at.% Al–Fe single crystal deformed to 4.0% strain.

Table 1. Number of neighbouring atoms around host Fe atom in $Fe_{(1+c)}Al_{(1-c)}$ with the B2 structure, before and after plastic deformation.

		Neighbouring atoms			
		Number of first NN atoms		Number of second NN atoms	
Host Fe atom		Fe	Al	Fe	Al
Normal state	Around α site	$8c$	$8(1-c)$	6	0
	Around β site	8	0	$6c$	$6(1-c)$
APB {110}	Around α site	$2+6c$	$6(1-c)$	$4+2c$	$2(1-c)$
	Around β site	$6+2c$	$2(1-c)$	$2+4c$	$4(1-c)$

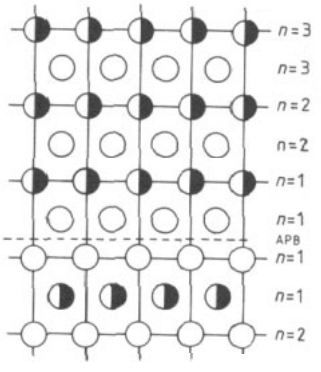

Figure 10. Schematic arrangement of Fe and Al atoms over the $(\bar{1}10)$ plane in the B2-type structure. α and β sites are represented by open circles and half full circles, respectively.

superlattice dislocations are distributed making pairs, which are called A-type superlattice dislocations in this paper. Then the numbers of α- and β-site Fe atoms per unit volume are given, respectively, as

$$N'_\alpha = (S^2 r_0/\sqrt{2}\,a^2)\rho \tag{1}$$

and

$$N'_\beta = (S^2 c r_0/\sqrt{2}\,a^2)\rho \tag{2}$$

where S is the degree of order, a is a lattice constant and r_0 (=35 nm) is the separation of superlattice dislocations or the width of an APB strip.

Another type of superlattice dislocation is possible, i.e. one which is distributed independently and is free from the attractive force of the APB. This type would appear mainly in the advanced deformation stage and is called the B-type superlattice partial dislocation. For the B-type superpartial, the numbers of Fe atoms become,

$$N'_\alpha = (\sqrt{2}\,S^2/a^2)\sqrt{\rho} \tag{3}$$

and

$$N'_\beta = (\sqrt{2}\,S^2 c/a^2)\sqrt{\rho}. \tag{4}$$

If the effects of the magnetic transition from paramagnetism to ferromagnetism are extended as far as the nth NN distance from the APB (see figure 10), the number N_i of ferromagnetically coupled Fe atoms is nN'_i. The net spontaneous magnetization of the plastically deformed Fe–Al alloys at 0 K can be written as,

$$M(0) = M_0 + N_\alpha(\mu'_\alpha - \mu_\alpha) + N_\beta(\mu'_\beta - \mu_\beta). \tag{5}$$

Here μ_α and μ_β are the magnetic moments of α- and β-site Fe atoms in the ordered state, respectively, and μ'_α and μ'_β are those in the vicinity of the APB. M_0 is the spontaneous magnetization before plastic deformation.

The above relations between $M(0)$ and ρ are shown in figure 11 in comparison with the experimental results. Here only the effect of A-type superlattice dislocation is considered and $\mu'_\alpha = \mu'_\beta = 2.2\,\mu_B$, $\mu_\alpha = \mu_\beta = 0$, $M_0 = 0$ and S is supposed to be 1. The calculated results are shown by full and broken lines, for 40.0 and 36.2 at.% Al contents, respectively, where the separations r_0 are 30 and 35 nm, respectively. The M_s values at 77 K are indicated by full circles (40.0 at.% Al–Fe) and open circles (36.2 at.% Al–Fe). The uncertainties in ρ are shown by error bars. The calculated and experimental results agree well, if one considers the extension of the magnetic transition to the greater distance from the APB with $n = 2$ or 3.

Figure 12 shows the relations between M_s and ρ in comparison with the experimental results of 34.0 at.% Al alloy. In the calculated results, $\mu'_\alpha = \mu'_\beta = 2.2\,\mu_B$, $\mu_\alpha = \mu_\beta = 0.2\,\mu_B$, $M_0 = 13.2 \times 10^{-2}$ Wb m^{-2} and $r_0 = 35$ nm are adopted. The values of M_s at 77 K are adopted in the experimental results. The comparison suggests that the magnetic influence of the APB on the neighbouring Fe atoms extends to much greater distances and n equals about 35, if one considers only the effect of A-type superlattice dislocations. As the width of the APB strip in B-type superlattice dislocations is much larger than in A-type dislocations, the existence of B-type dislocations would reduce the n value. Although B-type superlattice dislocations could be observed, especially in the advanced deformation stage, A-type superlattice dislocations predominate in the present specimens.

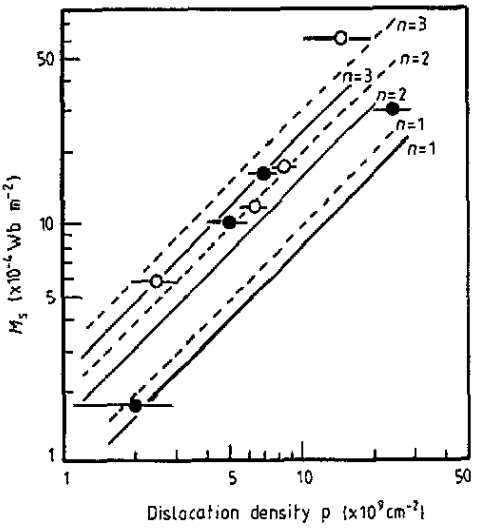

Figure 11. Comparison of experimental results (● and ○) and calculated results (—— and – – –) for the relation between the spontaneous magnetization M_s and ρ for 40.0 at.% Al–Fe (—— and ○) and 36.2 at.% Al–Fe alloys (– – – and ●).

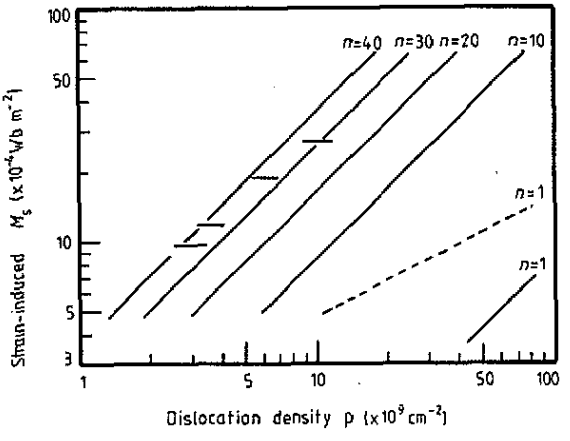

Figure 12. The relation between the strain-induced spontaneous magnetization M_s and ρ in comparison with the experimental results (segments of a line) for 34.0 at.% Al–Fe alloy. The full lines and broken line are the calculated results for A and B type superlattice dislocations, respectively.

5. Discussion

The atomic rearrangement in the vicinity of the APB brings about a considerable change in the magnetic properties; though one could not admit any change in the crystal structure except for the introduction of the APB strips, M_s appears and increases and χ augments after deformation. Huffman and Fisher (1967) obtained the relation between the moment value of an Fe atom and the atomic arrangement of the NN sites; the magnetic moment depends on n_{Al}. n_{Al} around the α-site Fe atoms in the vicinity of the APB is

4.8 and 4.4 in 40.0 at.% and 36.2 at.% Al contents, respectively (see table 1). The experimental value of M_s could not be explained only by the dependence on n_{Al}. Besnus *et al* (1975) explained the values of M_s and χ of heavily cold-worked Fe–Al alloys by a local environment model; the host Fe atom carries a moment only if surrounded by at least eight Fe atoms within the second NN cell. The number of Fe atoms around the host α- and β-site Fe atoms in the vicinity of the APB is the same as in the ordered state within the second NN cell (see table 1). Thus the appearance of M_s cannot be interpreted by the local environment model only. In the vicinity of the APB, the α-site Fe atoms are arranged in a chain with their first NN as shown in figure 10. The geometrical configuration of Fe atoms as well as n_{Al} plays an important role of the magnetic transition.

The experimental value of M_s at 77 K is about twice that of the calculated one at 36.2 and 40.0 at.% Al contents; $n = 2$ or 3. The effect of B-type superlattice dislocations would reduce the n-value, but electron microscopy observation shows that the A-type dislocation predominates. The chained ferromagnetic Fe atoms make the neighbouring Fe atoms magnetically enhanced and change them to ferromagnetic. Actually the magnetic influence would extend further than $n = 2$ or 3 for three reasons; first the value of M_s at 0 K would be larger than that at 77 K, secondly in the present calculation $S = 1$ is assumed, and thirdly the moment value of 2.2 μ_B is adopted for every ferromagnetic Fe atom.

The experimental value of M_s at 34.0 at.% Al content is about 35 times as large as the calculated one, when only the A-type superlattice dislocations contribute to plastic deformation. Actually many B-type superlattice dislocations are observed at 34.0 at.% Al content and they would reduce the difference between M_s values. However, the n value would become larger than 35 for the same reasons as discussed above. Considering these n values, the magnetic influence at 34.0 at.% Al content would be much longer range than at 36.2 and 40.0 at.% Al content. At the magnetically delicate composition, the extent of the magnetic influence is very sensitive to Fe content. Before plastic deformation, the atomic fluctuation would produce small ferromagnetic clusters and superparamagnetic clusters in the crystal (Cable *et al* 1977). When the APB strips are induced, the superparamagnetic cluster changes to ferromagnetic or mictomagnetic† at the delicate composition. The same idea has also been applied to the explanation of M_s in Pt_3Fe (Takahashi and Umakoshi 1990a).

M_s has a maximum at about 200 K in the 34.0 at.% Al–Fe alloy as a result of plastic deformation. A similar phenomenon was discovered by Danan and Gengnagel (1968); in the magnetization of the undeformed specimens with 29 to 33 at.% Al contents, a broad maximum was found at about 200 K. These two broad maxima near 200 K would be caused by the same effect. A displaced hysteresis loop was observed at 1.8 K in 30 at.% Al–Fe alloy, after being cooled to that temperature in a magnetic field (Kouvel 1959). Then the transition from ferromagnetism to mictomagnetism was investigated in detail near the 30 at.% Al composition and the freezing temperature, below which it becomes mictomagnetic, was determined by the alternating low-field susceptibility measurement made by Shull *et al* (1976). The broad maxima at near 200 K would be caused by mictomagnetism. A detailed study is now in progress.

The strong paramagnetic term in the heavily cold-worked Fe–Al alloys was also explained by the local environment model (Besnus *et al* 1975). But the increase of χ in

† The term mictomagnetism is used to designate the magnetic effects observed in alloys with spin orientations frozen at low temperatures but, in contrast to ferromagnetism and to antiferromagnetism, without long range magnetic order (Beck 1971).

the present specimens could not be interpreted by their model. In the 1.6% strained specimen with 40.0 at.% Al content, for example, the mean distance of APB strips is about 10^2 nm and excluding APB strips the crystal structure remains in the same atomic configuration as the undeformed one. The number of ferromagnetic Fe atoms in the vicinity of the APB would be about 10^{-2}% of the total Fe atoms. The long-range magnetic influence should be introduced as a reasonable explanation for the remarkable increase of χ. The ferromagnetic APB strips would exert a magnetic influence on the neighbouring Fe atoms as far as 10^2 nm and the Fe atoms are changed from paramagnetic to superparamagnetic. With increasing Fe contents near the critical composition, the influence extends further and becomes drastic.

M_s appears below T_C in the plastically deformed specimens, which would correspond to Curie temperature. T_C becomes high with increasing ε as shown in figures 4 and 5. The variation of T_C due to order–disorder processes in Fe–Al alloys was explained by Kouvel (1969) depending on the local atomic environment in which the relative number of the various exchange couplings in the NN was taken into account. Fe atoms in the vicinity of the APB make a ferromagnetic cluster with T_C. As the size of the APB strip and the atomic configuration in the vicinity of the APB strip are independent of ε at the initial deformation stage, the variation of T_C with ε or ρ cannot be explained by the local atomic environment. If there is no magnetic interaction between APB strips, T_C would be independent of ε and have a constant value. However, the experimental result is in conflict with this supposition. There exists some magnetic interaction between these magnetic clusters and T_C depends on the distance between the clusters. Electron microscopy shows that the mean distances of APB strips in the 1.6% and 3% strained specimens with 40.0 at.% Al content are about 2×10^2 nm and 1×10^2 nm, respectively. Also T_C increases from 80 to 110 K with increasing plastic strain from 1.6% to 3%. The magnetic interaction is a long-distance type attaining to at least 10^2 nm. Such a long-distance interaction is also observed in the dependence of χ on ε. It would point to the conclusion that there exists a long-distance interaction in the Fe–Al alloys which decides magnetic properties.

References

Beck P A 1971 *Metallogr. Trans.* **2** 2015
Besnus M J, Herr A and Meyer A J 1975 *J. Phys. F: Met. Phys.* **5** 2138
Cable J W, David L and Parra R 1977 *Phys. Rev.* B **16** 1132
Danan H and Gengnagel H 1968 *J. Appl. Phys.* **39** 678
Huffman G P and Fisher R M 1967 *J. Appl. Phys.* **38** 735
Kouvel J S 1959 *J. Appl. Phys.* **30** 313S
Kouvel J S 1969 *Magnetism and Metallurgy* vol 2 (New York: Academic) p 523
Leamy H J, Kayser F X and Marcinkowski M J 1969 *Phil. Mag.* **20** 763
Shull R D, Okamoto H and Beck P A 1976 *Solid State Commun.* **20** 863
Takahashi S 1986 *J. Magn. Magn. Mater.* **54–6** 1065
Takahashi S and Umakoshi Y 1990a *J. Phys.: Condens. Matter* **2** 2133
—— 1990b *J. Phys.: Condens. Matter* **2** 4007
Umakoshi Y and Yamaguchi M 1980 *Phil. Mag.* A **41** 573